BNL-107562-2015-JA

Elliptic and triangular flow in p+Pb and peripheral Pb+Pb collisions from parton scatterings

Adam Bzdak[1,2,*] and Guo-Liang Ma[3,†]

[1] RIKEN BNL Research Center, Brookhaven National Laboratory, Upton, NY 11973, USA
[2] AGH University of Science and Technology, 30-059 Krakow, Poland
[3] Shanghai Institute of Applied Physics, Chinese Academy of Sciences, Shanghai 201800, China

Using a multiphase transport model (AMPT) we calculate the elliptic, v_2, and triangular, v_3, Fourier coefficients of the two-particle azimuthal correlation function in proton-nucleus (p+Pb) and peripheral nucleus-nucleus (Pb+Pb) collisions. Our results for v_3 are in a good agreement with the CMS data collected at the Large Hadron Collider. The v_2 coefficient is very well described in p+Pb collisions and is underestimated for higher transverse momenta in Pb+Pb interactions. The characteristic mass ordering of v_2 in p+Pb is reproduced whereas for v_3 this effect is not observed. We further predict the pseudorapidity dependence of v_2 and v_3 in p+Pb and observe that both are increasing when going from a proton side to a Pb-nucleus side. Predictions for the higher order Fourier coefficients, v_4 and v_5, in p+Pb are also presented.

PACS numbers: 25.75.-q, 25.75.Gz, 25.75.Ld

Recently we argued [1] that the incoherent scattering of partons, as present in a multiphase transport model (AMPT) [2], with a modest elastic parton-parton cross-section $\sigma = 1.5 - 3$ mb, allows to understand qualitatively and quantitatively the long-range two-particle azimuthal correlation functions in proton-lead (p+Pb) and high-multiplicity proton-proton (p+p) collisions. Such correlations were recently observed by the CMS [3–5], ALICE [6, 7] and ATLAS [8, 9] Collaborations at the Large Hadron Collider (LHC), and by the PHENIX Collaboration in deuteron-gold collisions at the Relativistic Heavy Ion Collider (RHIC) [10].

Interestingly all features of the two-particle azimuthal correlation function observed in p+Pb collisions are very similar to those observed in A+A interactions, where such correlations are commonly attributed to the hydrodynamic expansion of the produced fireball. This naturally suggests that collective physics is present in p+A collisions [1, 11–17]. Particularly strong evidence in favour of hydrodynamics (or any other approach where the initial coordinate space anisotropy is transformed into the final momentum anisotropy) in p+A and peripheral A+A collisions is an approximate equality of multiparticle elliptic flow cumulants, $v_2\{4\} \approx v_2\{6\} \approx v_2\{8\}$, as predicted in Ref. [18], see also [19, 20], and confirmed recently by the CMS Collaboration [21]. Other strong evidence is the characteristic mass ordering of the elliptic flow, v_2, observed by the ALICE Collaboration in Ref. [7], and successfully reproduced by hydrodynamic calculations [22, 23].

The experimental data for the two-particle azimuthal correlation function can be also fitted within the color glass condensate framework [24], where the interesting part of the two-particle correlation function comes from the emission of two gluons in the so-called glasma diagram [25]. For a detailed discussion of this approach we refer the reader to Refs. [25–27].

It is important to clarify whether the signal in p+A collisions comes form the initial or final (or both) state effects. To this end several interesting observations were recently published [28–35] which could help to distinguish between competing models of p+A interactions. A simple conformal scaling argument, presented in Ref. [31], indicates a presence of a collective response to the geometry in p+Pb and Pb+Pb collisions.

In this Letter we focus on the detailed discussion of the elliptic and triangular coefficients of the two-particle azimuthal correlation function in p+Pb and peripheral Pb+Pb collisions. Qualitatively we reproduce all trends observed in the data. In particular, we find that v_2 in p+Pb is in a good agreement with the CMS data for a broad range of $N_{\rm track}$ and $p_{\rm T}$. In peripheral Pb+Pb collisions v_2 is underestimated for higher $p_{\rm T}$ and the integrated v_2 is 20% below the data (the model is not expected to work with better accuracy) however, the $N_{\rm track}$ functional dependence is well reproduced. As far as the v_3 coefficient [36] is concerned we obtain a good description of the data in both p+Pb and Pb+Pb collisions. We observe that the integrated v_3 is very similar in both systems for a broad range of $N_{\rm track}$. We further confirm the mass ordering of v_2 which is a characteristic feature of collective dynamics. Finally we predict the dependence of the two-particle correlation function on the pseudorapidity sum, $\eta_1 + \eta_2$, at a given pseudorapidity separation, $\eta_1 - \eta_2$, between two particles. We observe that v_2 and v_3 increase with the rapidity sum (that is when going towards a Pb fragmentation region), which is thought as a helpful probe to distinguish between various models of p+Pb collisions. We also predict the higher-order Fourier coefficients, v_4 and v_5, in p+Pb collisions and find them roughly a factor of 2 smaller than the v_3 coefficient.

Similar to our previous work we use the AMPT model with the string melting mechanism. In this model all initial minijets and soft strings are converted into quarks

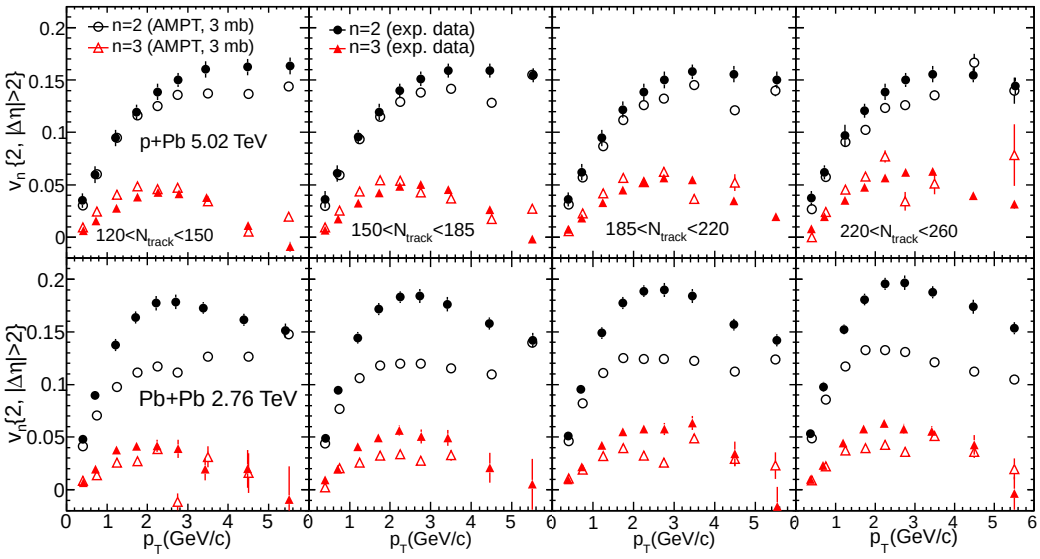

FIG. 1: The transverse momentum dependence of the elliptic, v_2, and triangular, v_3, flow coefficients in p+Pb (upper panel) and Pb+Pb collisions (lower panel) as obtained in the AMPT model (open symbols) with the string melting mechanism. Different centrality classes are defined by the number of produced charged particles, $N_{\rm track}$, measured in $|\eta| < 2.4$ and $p_{\rm T} > 0.4$ GeV/c. The CMS data are denoted by the full points.

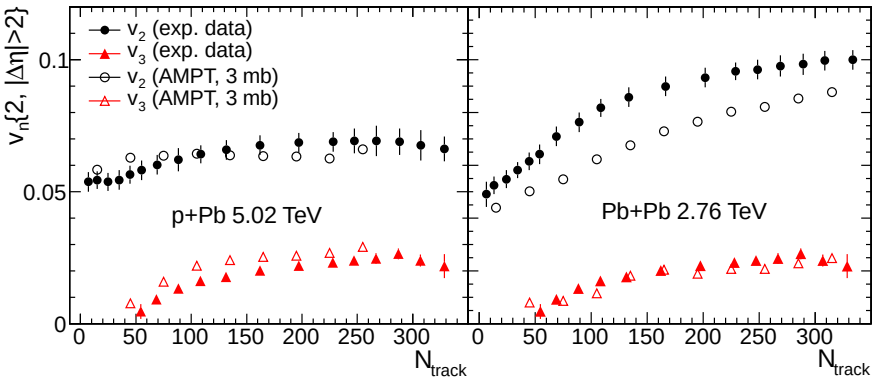

FIG. 2: The CMS data (full points) vs the AMPT model (open symbols) with the string melting mechanism for the integrated elliptic, v_2, and triangular, v_3, flow coefficients in p+Pb (left) and Pb+Pb (right) collisions as a function of the number of produced charged particles, $N_{\rm track}$, measured in $|\eta| < 2.4$ and $p_{\rm T} > 0.4$ GeV/c.

and antiquarks which undergo elastic scatterings (in contrast to the default model, where only partons from minijets interact) with a partonic cross-section which is controlled by the strong coupling constant and the Debye screening mass. Subsequently a simple coalescence model is employed to form hadrons which further undergo hadronic scatterings. The detailed description of the AMPT model can be found in Ref. [2]. The AMPT model provides a consistent framework to understand many phenomena in p+p, p+A and A+A collisions. In particular, different orders of harmonic coefficients have been well reproduced in Au+Au collisions at the top RHIC energy [37] and Pb+Pb collisions at the LHC energy [38], which indicates that in A+A interactions, the initial spacial asymmetry is transformed into the final momentum anisotropy via the incoherent parton scatterings [39].

In our previous study, the long-range two-particle azimuthal correlations have been observed in p+p and p+Pb collisions at the LHC energies with a modest parton-parton cross-section of $\sigma = 1.5 - 3$ mb [1]. Therefore, it is important to check if the flow coefficients v_n extracted from the long-range two-particle azimuthal correlation function are comparable with the data. In this work we simulate p+Pb collisions at $\sqrt{s} = 5.02$ TeV and peripheral Pb+Pb collisions $(50 - 100\%)$ at $\sqrt{s} = 2.76$ TeV with the parton-parton cross-section of 3 mb, being consistent with our previous study.

In Fig. 1 we present the elliptic and triangular Fourier coefficients from the long-range two-particle azimuthal

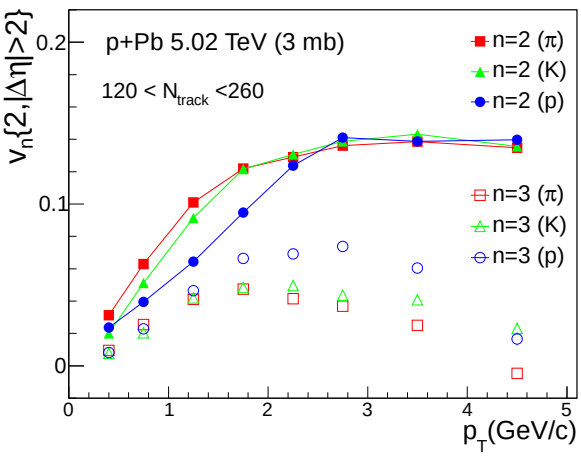

FIG. 3: The elliptic and triangular flow coefficients in p+Pb ($120 < N_{\rm track} < 260$) as a function of the transverse momentum for pions, kaons and protons as obtained in the AMPT model with the string melting mechanizm.

correlation functions, i.e. $v_n\{2, |\Delta\eta| > 2\}$, as a function of the transverse momentum, $p_{\rm T}$, in p+Pb (upper panel) and Pb+Pb collisions (lower panel) at $\sqrt{s} = 5.02$ TeV and 2.76 TeV, respectively. In our analysis we exactly follow the CMS procedure as described in Ref. [5]. The description of the p+Pb data is very good for both v_2 and v_3 in the whole available transverse momentum range and for various centrality classes defined by the number of produced charged particles, $N_{\rm track}$, measured in $|\eta| < 2.4$ and $p_{\rm T} > 0.4$ GeV/c. This is a nontrivial result suggesting that the AMPT model captures the main features of p+A physics. In Pb+Pb collisions v_3 is consistent with the data, within the error bars, and surprisingly v_2 is underestimated for $p_{\rm T} > 1$ GeV/c [40]. It is interesting to notice that $v_2(p_{\rm T})$ in Pb+Pb has a characteristic maximum around $p_{\rm T} = 2.5$ GeV/c which is not present in p+Pb data. On the contrary $v_3(p_{\rm T})$ is very similar in both systems and is well described by the AMPT model.

In Fig. 2 we present the integrated ($0.3 < p_{\rm T} < 3$ GeV/c) v_2 and v_3 for both p+Pb and Pb+Pb collisions. Again, v_2 and v_3 are very well described in p+Pb collisions for all available $N_{\rm track}$. Unfortunately, at present we cannot go to the highest values of $N_{\rm track} > 300$ to check whether v_3 starts decreasing as suggested by the data. In Pb+Pb collisions the integrated v_3 is consistent with the data for all $N_{\rm track}$ and the v_2 coefficient is underestimated by roughly 20%. It is worth noticing that within the AMPT approach the integrated v_3 in p+Pb and Pb+Pb interactions is roughly the same.

It is interesting to calculate $v_2(p_{\rm T})$ and $v_3(p_{\rm T})$ separately for pions, kaons and protons. The recently observed mass ordering of v_2 in p+Pb collisions serves as a crucial test of the initial vs the final state effects. In hydrodynamics we naturally obtain the mass ordering [22, 23] which is not obvious in the initial state scenarios. We checked that the mass ordering of v_2 is present in the AMPT model, as presented in Fig. 3. Interestingly we do not observe the mass ordering for v_3, being consistent with the calculations of Ref. [22].

We further present our predictions for the pseudorapidity dependence of the two-particle azimuthal correlation function in p+Pb collisions. In our calculations we take two narrow pseudorapidity bins with a given pseudorapidity separation $\Delta\eta = \eta_2 - \eta_1$. Next we shift both bins simultaneously across the pseudorapidity axis to study the azimuthal correlation function for various values of the pseudorapidity sum, $\Sigma\eta = \eta_1 + \eta_2$, at a given $\Delta\eta$. Schematically this situation is presented in Fig. 4. We calculate the two-particle azimuthal correlation function, $C(\Delta\phi)$, defined as

$$C(\Delta\phi) \equiv \frac{Y_{\rm Same}(\Delta\phi)}{Y_{\rm Mixed}(\Delta\phi)} \times \frac{\int Y_{\rm Mixed}(\Delta\phi) d\Delta\phi}{\int Y_{\rm Same}(\Delta\phi) d\Delta\phi} \qquad (1)$$

where $Y_{\rm Same}(\Delta\phi = \phi_2 - \phi_1)$ and $Y_{\rm Mixed}(\Delta\phi)$ are, respectively, the numbers of particle pairs (i.e. one particle is in bin 1 and the other particle is in bin 2) at a given $\Delta\phi$ and within a given $p_{\rm T}$ range. This definition of $C(\Delta\phi)$ removes a trivial dependence on the number of produced particles in both bins [41, 42].

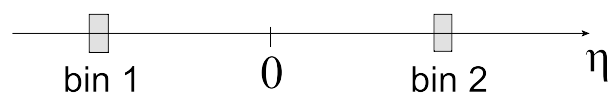

FIG. 4: Two narrow bins in pseudorapidity with $\Sigma\eta = \eta_1 + \eta_2 \sim 0$. We shift both bins simultaneously to study the dependence of $C(\Delta\phi)$ on $\Sigma\eta$ at a given $\Delta\eta = \eta_2 - \eta_1$.

In this exercise we calculate for p+Pb events with $N_{\rm track} > 110$ (measured in $|\eta| < 2.4$ and $p_{\rm T} > 0.4$ GeV/c) and for pairs of charged particles with $1 < p_{\rm T} < 2$ GeV/c. To illustrate the effect we choose five different $\Sigma\eta$ configurations for a given $\Delta\eta \sim 4$: (i) bins 1 and 2 are respectively given by $[-6.2, -5.8]$ and $[-2.2, -1.8]$ for $\Sigma\eta \sim -8$, (ii) $[-4.2, -3.8]$ and $[-0.2, 0.2]$ for $\Sigma\eta \sim -4$, (iii) $[-2.2, -1.8]$ and $[1.8, 2.2]$ for $\Sigma\eta \sim 0$, (iv) $[-0.2, 0.2]$ and $[3.8, 4.2]$ for $\Sigma\eta \sim 4$, and (v) $[1.8, 2.2]$ and $[5.8, 6.2]$ for $\Sigma\eta \sim 8$. In our calculations, a Pb nucleus is characterized by a positive η, which means that the increasing value of $\Sigma\eta$ corresponds to shifting towards a Pb fragmentation region.

To illustrate the effect we extract the second and the third Fourier coefficients of $C(\Delta\phi)$

$$C(\Delta\phi) = 1 + \sum_n 2v_n^2 \cos(n\Delta\phi) \qquad (2)$$

and plot them as a function of $\Sigma\eta$. This result is presented in Fig. 5. Both v_2 and v_3 increase gradually when going from a proton side to a Pb-nucleus side. This result is expected since on a Pb-going side we have significantly

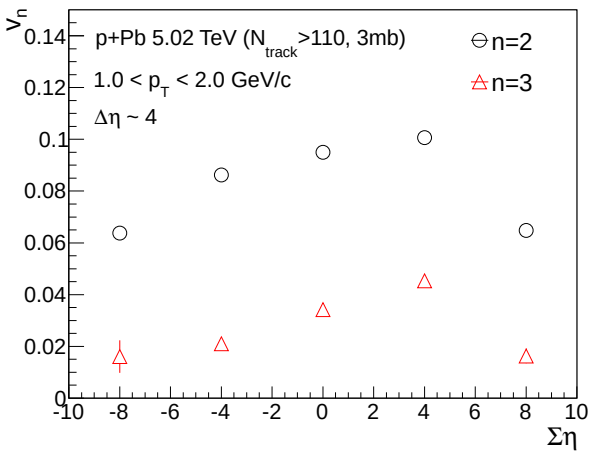

FIG. 5: The second and the third Fourier coefficients, as a function of the pseudorapidity sum $\Sigma\eta = \eta_1 + \eta_2$ at a given pseudorapidity separation $\Delta\eta \sim 4$. Increasing $\Sigma\eta$ corresponds to shifting towards a Pb-nucleus fragmentation region.

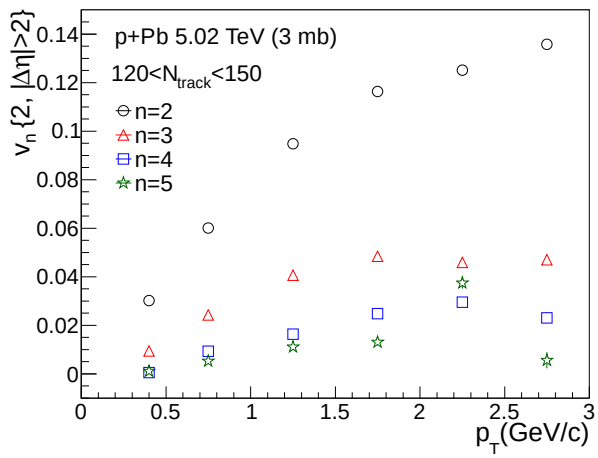

FIG. 6: The AMPT results for the two-particle azimuthal correlation function Fourier coefficients as a function of the transverse momentum in p+Pb collisions.

more produced partons and final particles. Another possible reason is the expected difference between the forward and backward eccentricities [43]. As expected, far in a nucleus fragmentation region both v_2 and v_3 start decreasing towards zero.

Finally, in Fig. 6 we present our predictions for the higher-order Fourier coefficients, v_4 and v_5, in p+Pb collisions. In the AMPT model with the string melting mechanism, both v_4 and v_5 are roughly a factor of 2 smaller than the v_3 coefficient. In our plot we only show the results for one centrality class $120 < N_{\rm track} < 150$ however, similar to v_2 and v_3 presented in Fig. 1, the results for v_4 and v_5 weakly change with different $N_{\rm track}$ classes.

Before concluding the paper we offer several comments.

Our results suggest that the incoherent scattering of partons plays an important role in the early stage of p+Pb and peripheral Pb+Pb collisions. Moreover, as discussed in Ref. [1], the AMPT model allows to understand the ridge effect in p+p for all measured $N_{\rm track}$ and $p_{\rm T}$. It is a nontrivial fact that all features present in the data can be qualitatively and quantitatively reproduced within a simple AMPT model.

We checked that the average number of elastic scatterings per parton is approximately 2 for $N_{\rm track} = 200$ in p+Pb, and changes monotonically with $N_{\rm track}$. We find it interesting that such a small number of collisions is sufficient to reproduce the data.

In our approach we assume that partons scatter incoherently. The lifetime of the partonic matter is roughly 1 fm/c (the time when partons stop interacting) and one could question the validity of this assumption. A simple estimate suggests that it is not unjustified. $\sigma = 3$ mb corresponds to the area of 0.3 fm^2. $N_{\rm track} = 200$ corresponds to roughly 40 particles per unit of rapidity and to the effective area per parton of ~ 0.1 fm^2 (we take the radius of p+Pb to be 2 fm). This number is of the same order of magnitude as σ indicating that in a parton's interaction area there are only a few partons (it is consistent with a small number of elastic scatterings), which makes our assumption plausible. The success of our approach could serve as an additional argument in favor of this assumption.

Finally we note that the effect of the hadronic cascade, which can be switched on and off in our approach, has a negligible effect on our results.

In conclusion, using the AMPT model with the string melting mechanizm, we investigated the elliptic and triangular Fourier coefficients of the long-range two-particle azimuthal correlation function in p+Pb and peripheral Pb+Pb collisions. In this model all initial minijets and soft strings are converted into partons which subsequently undergo elastic scatterings. This mechanizm allows us to understand various "flow" data measured in p+Pb and Pb+Pb collisions. In particular we obtained a good description of $v_2(p_{\rm T})$ and $v_3(p_{\rm T})$ in p+Pb for a broad range of the transverse momentum and for various centrality classes. The dependence of the integrated v_2 and v_3 on the number of produced charged particles, $N_{\rm track}$, is also nicely reproduced. In peripheral Pb+Pb collisions $v_3(p_{\rm T})$ and the integrated v_3 coefficients are in satisfactory agreement with the CMS data, however, v_2 is underestimated for higher transverse momentum resulting in 20% disagreement for the integrated v_2. We also verified the mass ordering of v_2 for pions, kaons and protons. We further predicted the pseudorapidity dependence of the two-particle azimuthal correlation function. We observed that v_2 and v_3 are gradually growing when going from a proton side to a Pb-nucleus side. Finally we calculated the higher-order Fourier coefficients, v_4 and v_5, in p+Pb collisions and found them to be about a factor of 2 smaller than the v_3 coefficient. We hope that the

results presented in this Letter will allow to disentangle between competing models of p+A collisions.

Discussions with L. McLerran and Sheng-Li Huang are appreciated. A.B. is supported through the RIKEN-BNL Research Center and grant No. UMO-2013/09/B/ST2/00497. G.-L. M. is supported by the Major State Basic Research Development Program in China under Grant No. 2014CB845404, the National Natural Science Foundation of China under Grants No. 11175232, No. 11375251, No. 11035009, and No. 11421505, the Knowledge Innovation Program of Chinese Academy of Sciences under Grant No. KJCX2-EW-N01, the Innovation Fund of Key Laboratory of Quark and Lepton Physics (Central China Normal University) under Grant No. QLPL2011P01, and the Shanghai Pujiang Program under Grant No. 13PJ1410600.

* Electronic address: abzdak@quark.phy.bnl.gov
† Electronic address: glma@sinap.ac.cn

[1] G. L. Ma and A. Bzdak, Phys. Lett. B **739**, 209 (2014).
[2] Z. -W. Lin, C. M. Ko, B. -A. Li, B. Zhang and S. Pal, Phys. Rev. C **72**, 064901 (2005).
[3] V. Khachatryan *et al.* [CMS Collaboration], JHEP **1009**, 091 (2010).
[4] S. Chatrchyan *et al.* [CMS Collaboration], Phys. Lett. B **718** (2013) 795.
[5] S. Chatrchyan *et al.* [CMS Collaboration], Phys. Lett. B **724**, 213 (2013).
[6] B. Abelev *et al.* [ALICE Collaboration], Phys. Lett. B **719**, 29 (2013).
[7] B. B. Abelev *et al.* [ALICE Collaboration], Phys. Lett. B **726**, 164 (2013).
[8] G. Aad *et al.* [ATLAS Collaboration], Phys. Rev. Lett. **110**, 182302 (2013).
[9] G. Aad *et al.* [ATLAS Collaboration], Phys. Lett. B **725**, 60 (2013).
[10] A. Adare *et al.* [PHENIX Collaboration], Phys. Rev. Lett. **111**, 212301 (2013).
[11] P. Bozek, Phys. Rev. C **85**, 014911 (2012).
[12] E. Shuryak and I. Zahed, Phys. Rev. C **88**, 044915 (2013).
[13] A. Bzdak, B. Schenke, P. Tribedy and R. Venugopalan, Phys. Rev. C **87**, no. 6, 064906 (2013).
[14] P. Bozek and W. Broniowski, Phys. Rev. C **88**, 014903 (2013).
[15] G. -Y. Qin and B. Mueller, Phys. Rev. C **89**, 044902 (2014).
[16] K. Werner, B. Guiot, I. Karpenko and T. Pierog, Phys. Rev. C **89**, 064903 (2014).
[17] I. Kozlov, M. Luzum, G. Denicol, S. Jeon and C. Gale, arXiv:1405.3976 [nucl-th].
[18] A. Bzdak, P. Bozek and L. McLerran, Nucl. Phys. A **927**, 15 (2014).
[19] L. Yan and J. -Y. Ollitrault, Phys. Rev. Lett. **112**, 082301 (2014).
[20] A. Bzdak and V. Skokov, arXiv:1312.7349 [hep-ph].
[21] CMS Collaboration, CMS Physics Analysis Summary No. CMS-PAS-HIN-14-006, 2014, http://cds.cern.ch/record/1705485
[22] P. Bozek, W. Broniowski and G. Torrieri, Phys. Rev. Lett. **111**, 172303 (2013).
[23] K. Werner, M. Bleicher, B. Guiot, I. Karpenko and T. Pierog, Phys. Rev. Lett. **112**, 232301 (2014).
[24] F. Gelis, E. Iancu, J. Jalilian-Marian and R. Venugopalan, Ann. Rev. Nucl. Part. Sci. **60**, 463 (2010).
[25] K. Dusling and R. Venugopalan, Phys. Rev. D **87**, 094034 (2013).
[26] Y. V. Kovchegov and D. E. Wertepny, Nucl. Phys. A **906**, 50 (2013).
[27] A. Kovner and M. Lublinsky, Int. J. Mod. Phys. E **22**, 1330001 (2013).
[28] A. Bzdak and V. Skokov, Phys. Lett. B **726**, 408 (2013).
[29] A. Bzdak and V. Skokov, Phys. Rev. Lett. **111**, 182301 (2013).
[30] P. Bozek, A. Bzdak and V. Skokov, Phys. Lett. B **728**, 662 (2014).
[31] G. Baar and D. Teaney, Phys. Rev. C **90**, 054903 (2014).
[32] V. P. Konchakovski, W. Cassing and V. D. Toneev, J. Phys. G **41**, 105004 (2014).
[33] A. M. Sickles, Phys. Lett. B **731**, 51 (2014).
[34] J. Noronha and A. Dumitru, Phys. Rev. D **89**, 094008 (2014).
[35] S. Floerchinger and U. A. Wiedemann, JHEP **1408**, 005 (2014).
[36] B. Alver and G. Roland, Phys. Rev. C **81**, 054905 (2010) [Erratum-ibid. C **82**, 039903 (2010)].
[37] L. Ma, G. L. Ma and Y. G. Ma, Phys. Rev. C **89**, 044907 (2014).
[38] J. Xu and C. M. Ko, Phys. Rev. C **84**, 044907 (2011).
[39] G. -L. Ma and X. -N. Wang, Phys. Rev. Lett. **106**, 162301 (2011).
[40] We checked that varying the cross-section in Pb+Pb only slightly improves the situation. At present we do not have an explanation why v_2 in Pb+Pb is underestimated. We can only speculate that it is related to the large average ellipticity present in peripheral Pb+Pb which could be underestimated in the Glauber model. Another possibility is some additional contribution to v_2, e.g., because of to an interplay of jet quenching and a strong elliptical shape of peripheral Pb+Pb.
[41] S. S. Adler *et al.* [PHENIX Collaboration], Phys. Rev. Lett. **97**, 052301 (2006).
[42] A. Adare *et al.* [PHENIX Collaboration], arXiv:1404.7461 [nucl-ex].
[43] J. Jia and P. Huo, Phys. Rev. C **90**, 034915 (2014).